Article:
Nourafkan, E (2018) Evaluation of adsorption of nonionic surfactants blend at water/oil interfaces. Journal of Dispersion Science and Technology, 39 (5). pp. 665-675. ISSN: 0193-2691

https://doi.org/10.1080/01932691.2017.1381618

Journal of Dispersion Science and Technology

ISSN: 0193-2691 (Print) 1532-2351 (Online) Journal homepage: http://www.tandfonline.com/loi/ldis20

Evaluation of adsorption of nonionic surfactants blend at water/oil interfaces

Ehsan Nourafkan

To cite this article: Ehsan Nourafkan (2017): Evaluation of adsorption of nonionic surfactants blend at water/oil interfaces, Journal of Dispersion Science and Technology, DOI: 10.1080/01932691.2017.1381618

To link to this article: http://dx.doi.org/10.1080/01932691.2017.1381618

Accepted author version posted online: 21 Sep 2017.

Evaluation of adsorption of nonionic surfactants blend at water/oil interfaces

Ehsan Nourafkan

School of Chemical and Process Engineering, University of Leeds, Leeds, UK

Address correspondence to Ehsan Nourafkan, School of Chemical and Process Engineering, University of Leeds, Leeds, LS2 9JT, UK. E-mail: e.nourafkan@leeds.ac.uk

ABSTRACT

The inherent biocompatibility of Span and Tween surfactants make them as an important class of nonionic emulsifiers which are employed extensively in emulsion and foam stabilization. The adsorption of Span-Tween blend at water/oil surface of emulsion has been investigated using a population balance model for the first time. Destability of emulsion was modeled by considering sedimentation, coalescence and interfacial coalescence terms in population balance equation (PBE). The terms of coalescence efficiency and interfacial coalescence time were considered as a function of surface coverage of droplets by surfactant molecules. The surface coverage at different surfactant concentrations was determined by minimization of difference between the model predictions and experimental average droplet sizes. After optimization, the surface coverage outputs were fitted with different adsorption isotherms to evaluate the adsorption behavior of Span-Tween surfactants blend at water/oil surface. The results show that Freundlich isotherm can predict the adsorption behavior of closer to the experimental observation. Moreover, fitted parameters imply the favorable adsorption of Span-Tween blend at water/oil interface.

GRAPHICAL ABSTRACT

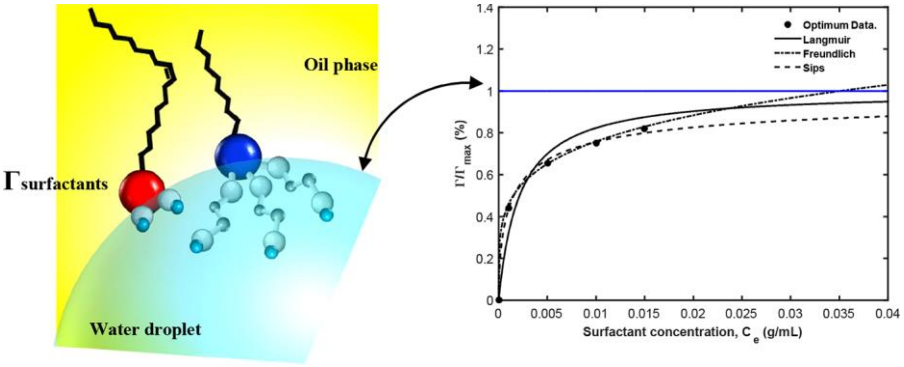

KEYWORDS: adsorption isotherm, population balance equation, surfactant coverage, water in oil emulsion

1. Introduction

Tween and span are important nonionic surfactants which are exploited for formation of emulsion in food industries,[1,2] pharmaceutical,[3,4] biomedical,[5] and remediation of oil floating on water.[6] There is a great interest in Tween-Span mixture because of synergistic effect of this blend for providing good dispersing ability as well as nontoxic and environmentally benign characterization. Posocco et al.[7] showed the synergistic effect of Span-Tween surfactants for emulsion formation. Nourfakan et al.[8] also used Tween-Span surfactants blend for synthesis of nanoparticles with different morphology in a microemulsion assisted media. The synergy between Span and Tween surfactants at molecular level schematically has been shown in **Figure 1**.

The head of Tween molecule has three hydrophilic oxyethylene chains which extend into water while Span molecule has a long hydrophobic tail which spreads in oil phase. Therefore, Span and Tween molecules match together and pack tightly at the surface of the water droplets in a continuous oil phase. The hydrocarbon tail of surfactant imparts steric stabilization to the water

droplets. In colloid science, the tendency of surfactant molecules adsorption at different surfaces is shown by adsorption isotherm. Generally, small-angle neutron scattering (SANS) is used as a reliable method for evaluation of adsorption isotherm at water/oil interface.[9,10] However, access to this type of facility is not possible for all researchers.

Awareness of surfactant adsorption isotherm at water/oil interface is valuable in wide variety of emulsion application from remediation of oil to synthesis of nanoparticles.[6,8] To the best of our knowledge, there were a few studies on evaluation of surfactant adsorption isotherm in emulsion, especially for Tween-Span mixture. In current research, we have developed a PBE model stand on relevancy of surfactant adsorption behavior and emulsion destability for the first time. The general framework of this idea has been illustrated in **Figure 2**.

The stability of the emulsion is dependent on adsorption of the surfactant molecules at the water/organic interface.[6,11] Kumar et al.[11] measured binary coalescence time of water drops in oil phase based on the surface coverage of droplets with surfactant molecules. Several mechanisms including coalescence, interfacial coalescence and settling of droplets occurred during the destabilization of emulsion, and they directly depend on adsorption surfactant molecules at water-oil interface. On the molecular level, the surfactant molecules remain bound to the surface of the water droplets, i.e., at the water/oil interface which reduces the interfacial tension between oil and water. The presence of bound molecules at the interface inhibits the coalescence of the droplets. Therefore, the coalescence function dependents on two main factors of droplets size distribution and degree of surfactant adsorption on interface. PBE can incorporate all the mechanisms involved during a sedimentation process, and hence it provide significant insight into the emulsion destabilization.[12,13]

Hartland and Jeelani[14–16] proposed a few mathematical models for the sedimentation of liquid dispersions, but were based on a single droplet size. Their models are acceptable to make rough estimations but cannot predict the effect of the droplets polydispersity on the coalescence and growth mechanisms in the emulsion zone. Grimes[17] conducted a comprehensive study on the modeling of batch gravity emulsion separation; the model considered the effect of dynamics of droplet contact and film drainage. The comparison of the modeling results with experimental data showed that the polydispersity of droplets was a main factor controlling the rate of coalescence droplets.

Not related to emulsion studies, Yang et al.[18] developed a PBM for the prediction of average polymorph content and aggregate size distribution of solid lipid nanoparticles. The model predicted the aggregation rate by using a first order correlation for particle's surface coverage with surfactant. The results clearly showed the change of surfactant surface coverage resulting in different particle size distribution of formed nanoparticles. Learning from the success of Yang et al.[18] this work modified the model that was proposed by Grimes[17] to predict the destabilization process and obtained surfactant adsorption isotherm by PBM in a water/nonionic surfactant/cyclohexane W/O emulsion.

2. Experimental Procedure

2.1. Material and characterization of W/O emulsions

The cyclohexane, sorbitane monooleate (Span 80) and polyethylene glycol sorbitan monolaurate (Tween 80) were purchased from Sigma-Aldrich. The variation of droplet size distribution (DSD) during the emulsion destabilization process was measured by using a Malvern Zetasizer. Five times of DSD measurement were conducted in each trial with 1 second time step

in between. A refractive index of 1.42, dielectric constant of 2.023 and viscosity of 0.93 centipoise for cyclohexane were used to calculate droplet size distributions. The behavior of emulsions with different surfactant concentrations were monitored by measuring the transmittance and backscattering of a pulsed near infrared light by Turbiscan Lab Expert, manufactured by Formulaction (France). An ultrasound generator (Fisher scientific Ltd.) was applied to provide the required energy for different emulsions synthesis. A D3300 Nikon camera (24 megapixel) set-up was used for the estimation of the height of coalescence water layer at bottom of column. The interfacial tension between de-ionized water and emulsion was measured using pendant drop method (CAM 2008, KSV instruments Ltd. Finland).

2.2. Preparation of emulsions

The nonionic mixture of Span 80 (oil soluble, HLB=4.3) and Tween 80 (water soluble, HLB=15) surfactants were selected for W/O emulsion formation. The weight percent of span 80/(span 80+tween 80) ratio was considered equal 20% according to result of our previous study.[19] Peltonen et al.[20] estimated the CMC of span surfactant was between 1.7-1.9×10^{-5} mol/lit (7.2-7.7×10^{-6} g/ml) for a wide range of nonpolar phase of Pentane to Dodecane. The CMC of Tween surfactant in nonpolar solvent is in order of 10^{-5}g/ml however there is not any CMC value for Tween surfactant in cyclohexane.[21] The surfactant concentrations for emulsion preparation was considered higher that 0.001 g/ml that is well above the CMC of both surfactants.

Four different emulsions including 70 ml cyclohexane, 5% volume percent water and 0.001, 0.005, 0.01, 0.015 g/ml surfactant concentrations were synthesis using ultrasound generator in a long glass column (**Figure 3**). The amplitude equal to 10 was applied to prevent the appearance of numerous nanodroplets that leads to long sedimentation time. The physicochemical properties

and sedimentation conditions are given in **Table 1. 1** ml of the suspension was collected from each level of sedimentation column for average size analysis (**Figure 3**). These samples were taken with the help of two syringes connected to needles with distinct length, enabling to take samples near the top and near the bottom of the vessel. The collected samples, then, were analyzed by Malvern zatasizer to measure the DSD. The sampling was performed every 30 minutes over a 6 hour period.

3. Model Formulation

3.1. Population balance equation

The unsteady-state batch settling model developed by Grimes[17] was used in this work. Some simplified assumptions were taken into account in the model:

- The wall effect was neglected.
- The droplets were initially homogeneously dispersed at the beginning of the settling, i.e., t = 0.
- The molecular diffusion of the dispersed phase was neglected (The destabilization by Ostwald ripening takes a long time which is important for nanoemulsion).
- The density of the dispersed phase remained constant everywhere in the settling column.

For such an unsteady state settling column, the PBM for the droplet size distribution can be described by the following equations.

$$\frac{\partial n(v,z,t)}{\partial t}+\frac{\partial}{\partial z}[U_z(v,z,t)n(v,z,t)]=B(v,z,t)-D(v,z,t)-R(v,z,t) \quad (1)$$

$$B(v,z,t)=\frac{1}{2[1-\phi(z,t)]}\int_0^v C(v',v,z,t)\,n(v-v',z,t)\,n(v',z,t)\,dv' \quad (2)$$

$$D(v,z,t)=\frac{n(v,z,t)}{1-\phi(z,t)}\int_0^{\infty}C(v',v,z,t)n(v',z,t)\,dv' \quad (3)$$

$$R(v,z,t)=\frac{n(v,z,t)}{\tau_{ic}}F(z-H_i(t)) \quad (4)$$

$$U_z(v,z,t)=\left[(\frac{3}{4\pi})^{2/3}\frac{2(\rho_d-\rho_c)g}{9\times10^4\mu_c}v^{2/3}\right] \quad (5)$$

$$\phi(z,t)=\int_0^{v_{max}}vn(v,z,t)dv \quad (6)$$

In Eq. 4, *F* is the Heavyside (step) function. The initial condition of Eq. 1 was set as the initial droplet size distribution, and the top boundary condition was obtained from the fact that the convective flux of droplets was zero at the top of the emulsion, as below.

$$n(v,0,z)=n_0(v) \quad (7)$$

$$n(v,t,0)=0 \quad (8)$$

3.2. Droplet coalescence

For coalescence between droplets, the coalescence frequency in Eq. 2 and 3 could be derived as the product of collision frequency and coalescence efficiency according to:

$$C(v',v,z,t)=\lambda(v',v,z,t)h(v',v) \quad (9)$$

The collision frequency of droplets was due to the Brownian coalescence and differential sedimentation coalescence according to the following coalescence rate function.[22]

$$h(v',v) = k_c(h_{Br} + h_{DS})$$
$$h_{Br}(v',v) = \left[\frac{2\times10^{12}k_BT}{3\mu_c}\frac{(v'^{1/3}+v^{1/3})^2}{v'^{1/3}v^{1/3}}\right]$$
$$h_{DS}(v',v) = \left[\frac{8\pi(\rho_d-\rho_c)g}{9\times10^4\mu_c}(v'^{1/3}+v^{1/3})^2\left|v'^{2/3}-v^{2/3}\right|\right] \quad (10)$$

In the literature, there are three theories that describe the coalescence process for droplets: film drainage model, energetic collision mechanism, and the critical approach velocity model. In this work, the modified film drainage model was used for coalescence efficiency development. It is considered that coalescence takes place in three main steps. First, two droplets (binary coalescence) approach and collide, resulting in a small amount of liquid trapped between droplets. Second, the interfacial film between the two droplets starts to drain to reach a critical thickness; and finally the interfacial film ruptures by van-der-Waals and other intermolecular forces, which leads to the merging of two droplets. The drainage of the interfacial thin film is a complex part of the coalescence mechanism, which was studied by several researchers.[23,24] The detail of film drainage theory is beyond the scope of this research and only briefly described here.

Jeelani and Hartland[25] developed the basic model for the coalescence time of droplets during the sedimentation and creaming process based on film drainage theory. The model incorporated the interfacial tension gradient when surfactant molecules were adsorbed at the interfaces. One complexity of the Hartland model is the difficulty of estimating the interfacial tension gradient at the periphery of droplets. Instead of Hartland's model the Henschke's model[26] is more complete and applicable by considering the effect of Van-der-Waals attraction between droplets. According to these different models, the coalescence efficiency for gravity sedimentation is a function of viscosity, density, Hamaker constant and interfacial tension as follows:

$$\lambda = \exp\left(-\frac{drainage\,time}{contact\,time}\right) = \exp\left[\mu_c, \Delta\rho, \gamma(C_S), H_{am.}(C_S)\right] \quad (11)$$

Assuming a constant viscosity and density of oil phase in column, Eq. 11 depends on the concentration of surfactant to estimate the tendency of two droplets to coalescence when the surface coverage is below the maximum coverage. In this study, the effect of concentration on Hamaker constant, interfacial tension was included in droplet coverage by surfactant. By considering the contact time as a constant and lumped to parameter K (s) equal 0.1,[17] the following expression was used to calculate coalescence efficiency:

$$\lambda(v', v) = \exp(-\tau_c) = \exp\left(-\frac{(\rho_d - \rho_c) g \mu_c}{K(1-\Gamma/\Gamma_{\max})^{\alpha} \gamma^{3/2} H_{am.}^{\;1/2}} \left(\frac{v'^{1/3} v^{1/3}}{v'^{1/3} + v^{1/3}}\right)^4\right) \quad (12)$$

The interfacial coalescence time (τ_{ic}) can be obtained from Eq. 12 when $v' \to 0$ and α was estimated using optimization. The Hamaker coefficient can be estimated experimentally, but in this study the value was fixed as 10^{-9}, similar to many other studies.[26] The interfacial tension was referred to the interfacial tension between pure cyclohexane and water. The interfacial coalescence is the interface between the third and last layer in which droplets are dissolved in water phase according to Eq. 4. The coalescence of droplets in the continuous phase depends on the surfactant layer coverage over the droplets. The position of the interfacial coalescence can be calculated from the overall mass balance of the dispersed phase, as the following:

$$\int_0^H \phi(z, t=0) dz = \int_0^t \int_0^{H_i(t)} \int_0^{v_{\max}} vR(v, z, t) dv dz dt + \int_0^{H_i(t)} \phi(z, t) dz \quad (13)$$

As the total initial water volume in the column is known and the total resolved water at the specific time *t* can be calculated via the integration of depth of droplets due to interfacial coalescence, which is specified over time.

3.3. Model solution

Several methods are available to solve the population balance equations such as moment transformation, finite difference, Laplace and Fourier transformations. There are also some numerical methods available for more complex population equation models.[27,28] Similar to our previous studies, the finite difference method (FDM) was used in this work to solve the population and mass balance equations.[29] The accuracy of the numerical solution by FDM increases as the number of size and time intervals increase at the cost of increased CPU time. Based on some trial and error calculations, the time increment step, height increment step and droplet size increment step were considered equal 30 s, 250 μm and 10 nm respectively in the FDM in this work.

The model solution can predict the DSD during the course of sedimentation at different times and different heights of the column. In order to solve the model equation, it is necessary that the empirical parameters are fully established. The optimum values of parameters were estimated by minimizing the deviations between the model predictions of average droplet sizes and those measured experimentally. Therefore, the optimal sets of parameters were found by solving the nonlinear optimization of the following objective function:

$$\theta = [k_c, \alpha, \Gamma / \Gamma_{\max}]$$

$$\Phi(\theta) = \sum_{i=1}^{N_e} \left[\sum_{j=1}^{N_D} \left[\left| \frac{\bar{D}_{\exp}(j) - \bar{D}_{\mathrm{mod}}(j)}{\bar{D}_{\exp}(j)} \right| \right] \right] \quad (14)$$

Note that the $[k_c,\alpha]$ parameters remain constant but the $[\Gamma/\Gamma_{max}]$ parameter changes for samples with different surfactant concentrations. The programming and optimization were performed in Matlab 7 software.

3.4. Surfactant adsorption isotherm

The nature of the adsorption isotherm strongly depends on the type of surfactant and emulsion characterization.[30,31] The adsorption isotherm and CMC of the W/O emulsion were obtained by PBM model and fitted adsorption isotherm. The optimum data of surface coverage of the droplet (Γ/Γ_{max}) for several surfactant concentrations were fitted with Langmuir, Freundlich and Sips adsorption isotherm according to Eq. 15-17.[32–34] The CMC of model was validated with experimental CMC that obtained was experimentally.

$$\Gamma/\Gamma_{\max} = \frac{K_L C_S}{1 + K_L C_S} \quad (15)$$

$$\Gamma/\Gamma_{\max} = K_F C_S^{1/m_F} \quad (16)$$

$$\Gamma/\Gamma_{\max} = \frac{K_S C_S^{m_S}}{1 + K_S C_S^{m_S}} \quad (17)$$

The Freundlich constant ($1/m_F$) is related to the adsorption intensity of the adsorbent. For $0.1 < 1/m_F < 0.5$, adsorption is favorable, and for $1/m_F > 1$, it is difficulty to adsorb.

4. Result and Discussion

4.1. Interfacial coalescence layer measurement

Generally with the passing of time, three layers were formed in the sedimentation column as schematically depicted in **Figure 4**.

A clear layer that is formed at the top of the sedimentation column contains very small nanodroplets. In the second layer, the coalescence and sedimentation mechanisms happen. The last layer is the sediments of disperse phase (here water) where the droplets have coalesced into a continuous phase. The estimation of height of interfacial coalescence layer using turbiscan is

difficult because of intense turbidity of emulsion just after mixing. The estimation of height of interfacial coalescence layer was performed using glass pipette (4 mm ID) test which is shown in **Figure 5a**. For this purpose the pipette was filled by emulsion till the height of solution inside pipette was equal to height of solution in main sedimentation column. Before filling pipette with emulsion, 200 µl de-ionized water was injected to pipette to produce a base level (**Figure 5a**). High resolution photos were captured (every 15 min) using camera and were used for estimation height of coalescence layer at the bottom of glass pipette during sedimentation process.

Figure 5b represents the change of interfacial coalescence layer by passing time. The final time of sedimentation process was estimated using turbiscan analysis when the difference between the final transmission heights became less than 0.1%. The height of samples was considered equal 50 mm because of limitation of sample place volume in turbiscan device. **Figure 5b** shows the transmission curves of emulsion containing 0.005 g/ml surfactant (i.e., changes in light intensity passing through the reverse emulsion).

4.2. Optimum kinetic parameters

The coalescence frequency, collision frequency, and coalescence efficiency at the start of sedimentation process for emulsion containing 0.005 g/ml surfactant concentration have been shown in **Figure 6**. It can be observed from **Figure 6a** that the large number of collisions among the large-small size droplets and the lower number of collisions among small-small and large-large droplets.

The coalescence efficiency adjusts the shape of collision frequency via droplets coverage surface. The effect of surface coverage of droplets on coalescence efficiency has been shown in **Figure 7**.

The optimum value of the model kinetic parameters have been reported in **Table 2**.

Figure 8 shows the change of average droplet sizes which were measured by DLS analysis, and those were obtained by the model predictions after emulsion immobility.

According to **Figure 8**, an increase in the average droplet size was observed at the beginning of the sedimentation process of emulsion containing 0.001 and 0.005 g/ml surfactant. This is due to the dominance of droplet coalescence over the sedimentation rate of droplets. The average droplet size was changed by two main factors of coalescence of droplets inside the column and interfacial coalescence of droplets on moving layer of water. The interfacial coalescence causes disappearance of large droplets in sedimentation column that decreases the average droplet size, while coalescence of droplets increase average droplet size. The rise of droplets size will be continued till the interfacial coalescence overcomes the coalescence of droplets.

Figures 9 shows the local volume fraction of water phase as a function of surfactant concentration and axial position in the column. As it can be seen from **Figure 9a**, the higher local volume fraction means that the enclosed area of emulsion is filled with droplets. The intersection of local volume fraction curves with other concentration is due to the different polydispersity of droplet size distribution which affect on coalescence efficiency of droplets.

As an instance, the intersections of curve for emulsion containing 0.001 g/ml surfactant, with other curves shows a higher local volume fraction at the top of the column. Different polydispersity of water droplet affects the coalescence efficiency which terminates the appearance of more droplets at top of column for lower surfactant concentration. The results indicated that a wide local volume fraction appeared inside column when the standard deviation of the droplet size distribution was increased. **Figure 9b** depicts the local volume fraction of emulsion containing

0.005 g/ml surfactant as a function of time. The results of model shows that more than 70% of water separated during four hours of sedimentation (about one fifth of total sedimentation time).

4.3. Fitting of adsorption isotherm and comparison with experimental data

The optimum data of the surface coverage of droplets at different surfactant concentrations (**Table 2**) were fitted by Langmuir, Freundlich and Sips isotherm adsorption. The results of fitting have been represented in **Table 3** and **Figure 10**. The value of regression coefficient (R^2) was found to be 0.988 for Sips and Freundlich, which indicates that both models have acceptable accuracy for fitting data. However, the prediction of complete monolayer coverage of droplets in continuous oil phase is different for Sips and Freundlich isotherms. Freundlich isotherm shows the complete monolayer coverage of droplets isotherm at surfactant concentration equal to 0.035 g/ml. The parameter *1/n equal* 0.219, in Freundlich isotherm shows that favorable adsorption on Span-Tween surfactant blend at W/O interface of emulsion. Generally, surfactant adsorption obeys Langmuir isotherm behavior;[9,10] however, the results of optimization for Tween-Span mixture in this study shows higher tendency of this blend for adsorption on W/O interface compare to Langmuir isotherm.

In order to validate the predicted complete monolayer coverage with experimental data, several water-in-oil emulsions were prepared at higher concentration of surfactants <0.015 g/ml (**Figure 11**). According to **Figure 11**, emulsions containing lower surfactant concentration were turbid that imply existence of large water droplets. The color of emulsions became more transparent by increasing the surfactant concentration which means higher droplets coverage, reducing interfacial tension and formation smaller water droplets. The average droplets size of emulsions versus surfactant concentrations is shown in **Figure 11b**. According to **Figure 11b**, the

minimum average droplet size is 77 nm which was obtain at 0.03 g/ml surfactants concentration. By addition of surfactants, the average droplet size was remained constant which imply the extra surfactant molecules remained at bulk of oil or water phase. In fact, the complete monolayer of droplets occured at surfactants concentration between 0.03-0.035 g/ml which is near to Freundlich isotherm prediction.

The interfacial tension data were determined using a pendant drop tensiometer as shown in **Figure 12**. According to **Figure 12**, IFT for emulsion containing surfactant concentrations below <0.025 g/mol is almost constant. However, at higher surfactant concentrations (0.03 g/ml<), the pendant drop method failed and a filament, instead of a drop, appeared (**Figure 13d**).[7] In fact, the surfaces of pendant droplet can be unstable due to accumulation of surfactant molecules in bulk of emulsion and thinning Van-der-Waals interactions. Therefore, the viscoelastic surface is ruptured and a thin filament is formed.

5. Conclusions

We have estimated the adsorption of tween-span surfactants blend at the water-oil interface using destability modeling of W/O emulsion. The main conclusions of the research may be summarized in the following points:

- Modeling of destability of emulsion could be used as a method for evaluation of surfactant adsorption on W/O interface.
- The optimum coverage of droplet surface with surfactant was fitted with some well-known adsorption isotherms. Generally, surfactants obey Langmuir isotherm trend however the results of this study shows that Freundlich and Sips models had more

accuracy for Span-Tween blend compare to Langmuir isotherm. Probably this is due to synergic effect of between Span-Tween surfactant molecules.

- The coefficients of determination for Freundlich and Sips fitting models were similar; however, predictions were different for complete surfactants coverage of water droplets in emulsion. The Freundlich prediction was closer to experimental observation. Moreover, the parameters of Freundlich imply favorable adsorption of span-tween blend on W/O interface.

Abbreviation and Nomenclature (Unit)

B Birth function ($\#\mu m^{-3}s^{-1}$)

C Coalescence kernel ($\mu m^{3}s^{-1}$)

C_s Surfactant concentration (g/ml)

CMC Critical micelles concentration (-)

D Death function ($\#\mu m^{-3}s^{-1}$)

$\bar{D}$ Average droplets diameter (μm)

DSD Droplet size distribution (μm)

F Step function (-)

g Gravitational acceleration, equal to 980 (cms^{-2})

H_i Height of the resolved dispersed phase layer (μm)

$H_{am.}$ Hamaker coefficient ($gm^{2}s^{-2}$)

h Collision frequency ($\mu m^{3}s^{-1}$)

h_{Br} Brownian coalescence ($\mu m^3 s^{-1}$)

h_{DS} Differential sedimentation coalescence ($\mu m^3 s^{-1}$)

j Counter of average droplet size (-)

i Counter of sample with different surfactant value (-)

k_B Boltzmann constant, equal to 1.38×10^{-16} ($cm^2 g s^{-2} K^{-1}$)

k_c Empirical fitting parameter of coalescence rate coefficient (-)

K_L Langmuir equilibrium constant (mL/g)

K_S Sips equilibrium constant $(mL/g)^m$

K_F Freundlich equilibrium constant (g/ml)

m_s Empirical constant in Sips equation (-)

m_F Empirical constant in Freundlich equation (-)

n Droplet population density ($\#\mu m^{-3}$)

n_0 Initial droplet population density

($\#\mu m^{-3}$)

N_D Number of measurement average droplet size (-)

N_e Number of samples with different surfactant amount (-)

R Rate of death of droplets due to interfacial coalescence ($\#\mu m^{-3} s^{-1}$)

t Time (s)

U_z Sedimentation velocity of a droplet (μms^{-1})

v Droplet volume (μm^3)

v` Droplet volume (μm^3)

z Axial coordinate and is

(μm)

Greek letter

Γ Surface coverage of the droplet ($molcm^{-2}$)

Γ_{max} Maximum surface coverage of the droplet ($molcm^{-2}$)

τ_{ic} Interfacial coalescence time (s)

φ Local volume of the dispersed phase in the emulsion at any position and time (μm^3#)

Φ Objective function (-)

ρ_d Density of disperse phase (gcm^{-3})

ρ_c Density of continues phase (gcm^{-3})

μ_c Dynamic viscosity of the continuous phase ($gcm^{-1}s^{-1}$)

λ Coalescence efficiency (-)

γ Interfacial tension ($g.s^{-2}$)

Acknowledgement

This work was supported by European Research Council Consolidator Grant (Grant number: 648375).

Notes

The authors declare no competing financial interest.

References

[1] Serdaroglu, M.; Ozturk, B.; Kara, A. *Turk. J. Agric.-Food Sci. Technol*. **2015**, *3*, 430–438.

[2] Woodward, N. C.; Gunning, A. P.; Mackie, A. R.; Wilde, P. J.; Morris, V. P. *Langmuir* **2009**, *25*, 6739–6744.

[3] Nielloud, F. *Pharmaceutical Emulsions and Suspensions*, 2nd ed.; CRC Press: Boca Raton, 2000.

[4] Bhattacharjee, J.; Verma, G.; Aswal, V. K.; Dale, A. A.; Nagarsenker, M. S.; Hassan, P. A. *J. Phys. Chem. B* **2010**, *114*, 16414–16421.

[5] Webb, S. D.; Cleland, J. L.; Carpenter, J. F.; Randolph, T. W. *J. Pharm. Sci.* **2002**, *91*, 543–558.

[6] Athas, J. C.; Jun, K.; McCafferty, C.; Owoseni, O.; John, V. T.; Raghavan, S. R. *Langmuir* **2014**, *30*, 9285–9294.

[7] Posocco, P.; Perazzo, A.; Preziosi, V.; Laurini, E.; Pricl, S.; Guido, S. *RSC Adv.* **2016**, *6*, 4723–4729.

[8] Nourafkan, E.; Asachi, M.; Gao, H.; Raza, G.; Wen, D. *J. Ind. Eng. Chem.* **2017**, *50*, 57–71.

[9] Staples, E.; Penfold, J.; Tucker, I. *J. Phys. Chem. B* **2000**, *104*, 606–614.

[10] Penfold, J.; Thomas, R. K.; Li, P. X.; Petkov, J. T.; Tucker, I.; Webster, J. R. P.; Terry, A. E. *Langmuir* **2015**, *31*, 3003–3011.

[11] Kumar, M. K.; Mitra, T.; Ghosh, P. *Ind. Eng. Chem. Res.* **2006**, *45*, 7135–7143.

[12] Cunha, R. E. P.; Fortuny, M.; Dariva, C.; Santos, A. F. *Ind. Eng. Chem. Res.* **2008**, *47*, 7094–7103.

[13] Abeynaike, A.; Sederman, A. J.; Khan, Y.; Johns, M. L.; Davidson, J. F.; Mackley, M. R. *Chem. Eng. Sci.* **2012**, *79*, 125–137.

[14] Hartland, S.; Jeelani, S. A. K. *Chem. Eng. Sci.* **1987**, *42*, 1927–1938.

[15] Hartland, S.; Jeelani, S. A. K. *Chem. Eng. Sci.* **1988**, *43*, 2421–2429.

[16] Jeelani, S. A. K.; Hartland, S. *J. AlChE* **1985**, *31*, 711–720.

[17] Grimes, B. A. *J. Dispers. Sci. Technol.* **2012**, *33*, 578–590.

[18] Yang, Y.; Corona, A.; Henson, M. A. *J. Colloid Interface Sci.* **2012**, *374*, 297–307.

[19] Nourafkan, E.; Hu, Z.; Gao, H.; Wen, D. *Chem. Eng. Res. Des.* **2017**. (submitted to).

[20] Peltonen, L.; Hirvonen, J.; Yliruusi, J. *J. Colloid Interface Sci.* **2001**, *240*, 272–276.

[21] Yeom, I.; Ghosh, M.; Cox, C.; Robinson, K. *Environ. Sci. Technol.* **1995**, *29*, 3015–3021.

[22] Reddy S. R.; Folger, H. S. *J. Colloid Interface Sci.* **1981**, *79*, 105–113.

[23] Chan, D. Y. C.; Klaseboer, E.; Manica, R. *Soft Matter* **2011**, *7*, 2235–2264.

[24] Choi, S. B.; Lee, J. S. *Microfluid. Nanofluid.* **2014**, *17*, 675–681.

[25] Jeelani, S. A. K.; Hartland, S. *J. Colloid Interface Sci.* **1994**, *164*, 296–308.

[26] Henschke, M.; Schlieper, L. H.; Pfennig, A. *Chem. Eng. Sci.* **2002**, *85*, 369–378.

[27] Bennett, M. K.; Rohani, S. *Chem. Eng. Sci.* **2001**, *56*, 6623–6633.

[28] Lim, Y. I.; Lann, J. M. L.; Meyer, X. M.; Joulia, X.; Lee, G.; Yoon, E. S. *Chem. Eng. Sci.* **2002**, *57*, 3715–3732.

[29] Nourafkan, E.; Alamdari, A. *J. Chem. Eng. Jpn.* **2009**, *42*, 231–240.

[30] Stumm, W.; Morgan, J. J. *Aquatic Chemistry: An Introduction Emphasizing Chemical Equilibria in Natural Waters*; J. Wiley and Sons: New York, 1970.

[31] Wei, X.; Wang, X.; Liu, J.; Sun, D.; Yin, B.; Wang, X. *Appl. Surf. Sci.* **2012**, *261*, 237–241.

[32] Langmuir, I. *J. Am. Chem. Soc.* **1916**, *38*, 2221–2295.

[33] Samiey, B.; Dargahi, M. *Cent. Eur. J. Chem.* **2010**, *8*, 906–912.

[34] Anirudhan, T. S.; Senan, P. *Chem. Eng. J.* **2011**, *168*, 678–690.

Table 1. The physicochemical properties of materials, sedimentation conditions and some model parameters that were used in the optimization process.

Properties	Value
Density of cyclohexane (gcm^{-3})	0.779
Density of water (gcm^{-3})	1
Viscosity of cyclohexane ($gcms^{-1}$)	0.0093
Interfacial tension of cyclohexane with water ($g.s^{-2}$) at 294.15 K	43.84
Initial water volume fraction	5%
Absolute temperature (K)	295.15
Diameter of sample column (mm)	30

Table 2. The optimum value of kinetic parameters for emulsion destability.

Parameter	k_c (–)	α (–)	C_e (g/mL cyclohexane)	Γ/Γ_∞	t_f (Day:hour)
Value	5.58×10^{-13}	1.4	0.001	0.44	0:16
			0.005	0.65	0:22
			0.01	0.76	1:18
			0.015	0.82	3:16

Table 3. The parameters of fitted isotherm adsorption models.

Isotherm model	Parameter	Value
Langmuir	K_L (L/g)	466
	R^2	0.941
	Adjusted R^2	0.941
Freundlich	K_F (mL/g)	2.08
	n	4.55
	R^2	0.998
	Adjusted R^2	0.998
Sips	K_S (mL/g)^m	51.69
	m	0.61
	R^2	0.998
	Adjusted R^2	0.997

Figure 1. Synergy between Span and Tween molecules at water/oil interface.

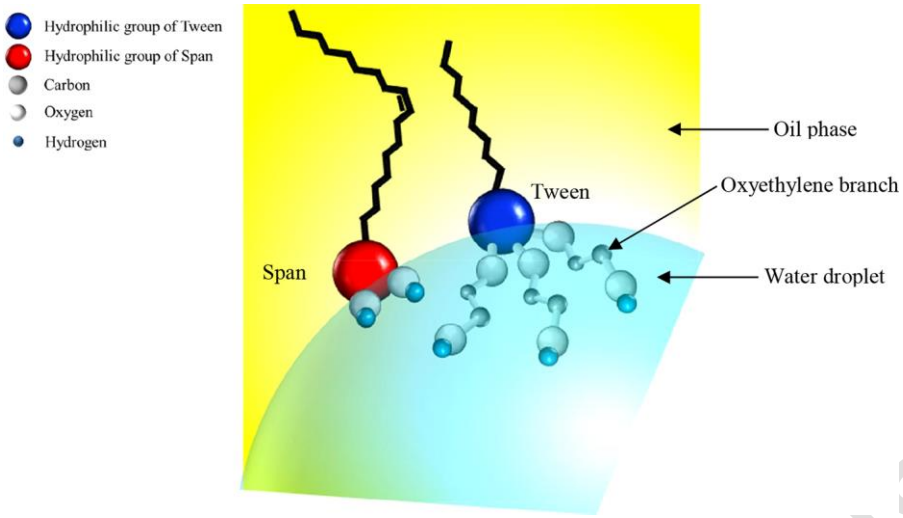

Figure 2. The general framework of this study.

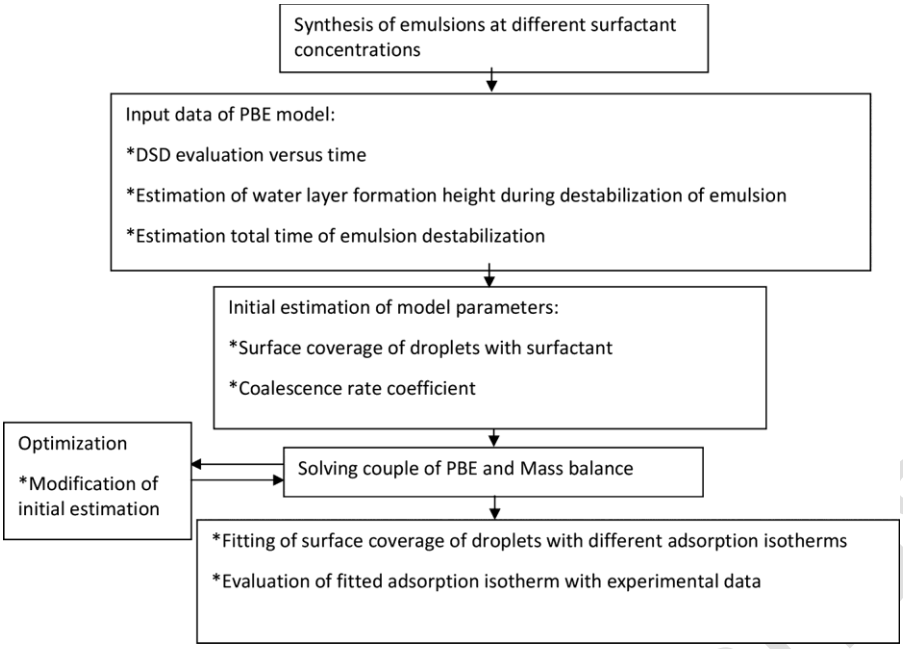

Figure 3. Sampling length from the sedimentation column.

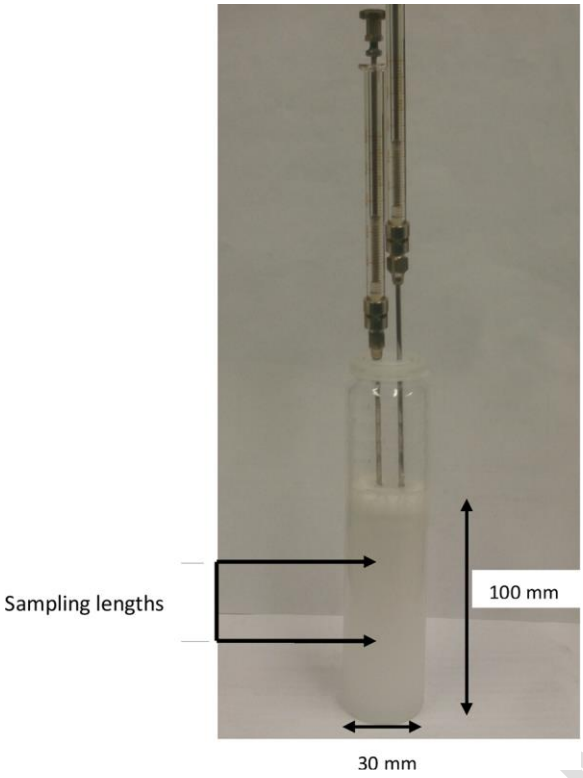

Figure 4. Schematic diagram of a sedimentation process under gravity for a reverse emulsion.

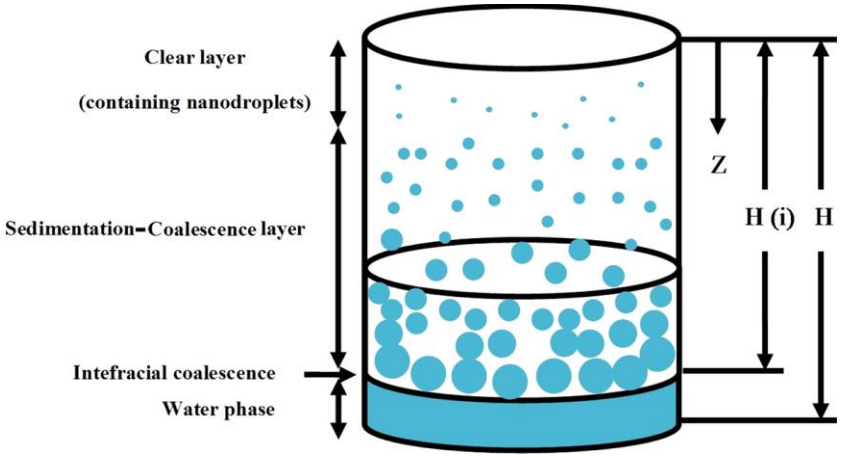

Figure 5. (a) Estimation of coalescence layer height using glass pipette, (b) Change of interfacial coalescence layer by passing time at different surfactant concentration, (c) transmission curves of emulsion containing 0.005 g/ml surfactant.

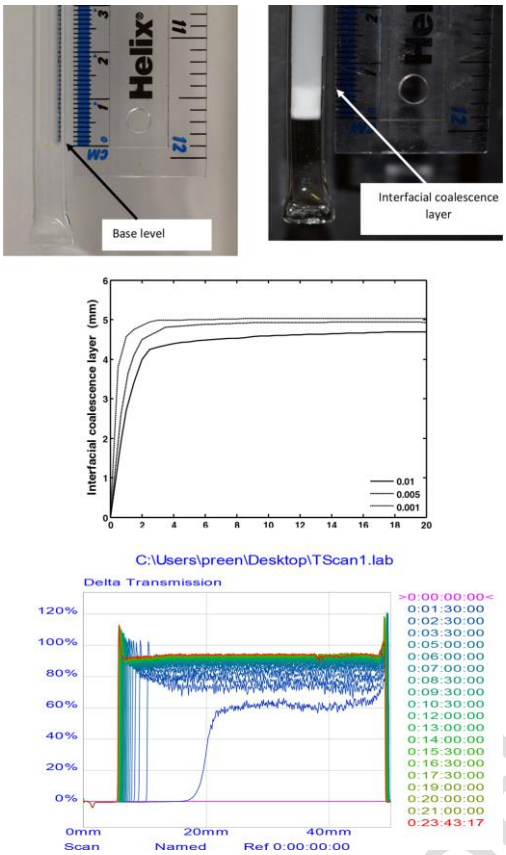

Figure 6. (a) Collision frequency, (b) coalescence efficiency, and (c) coalescence kernel of water droplets at 0.005 g/ml surfactant concentration.

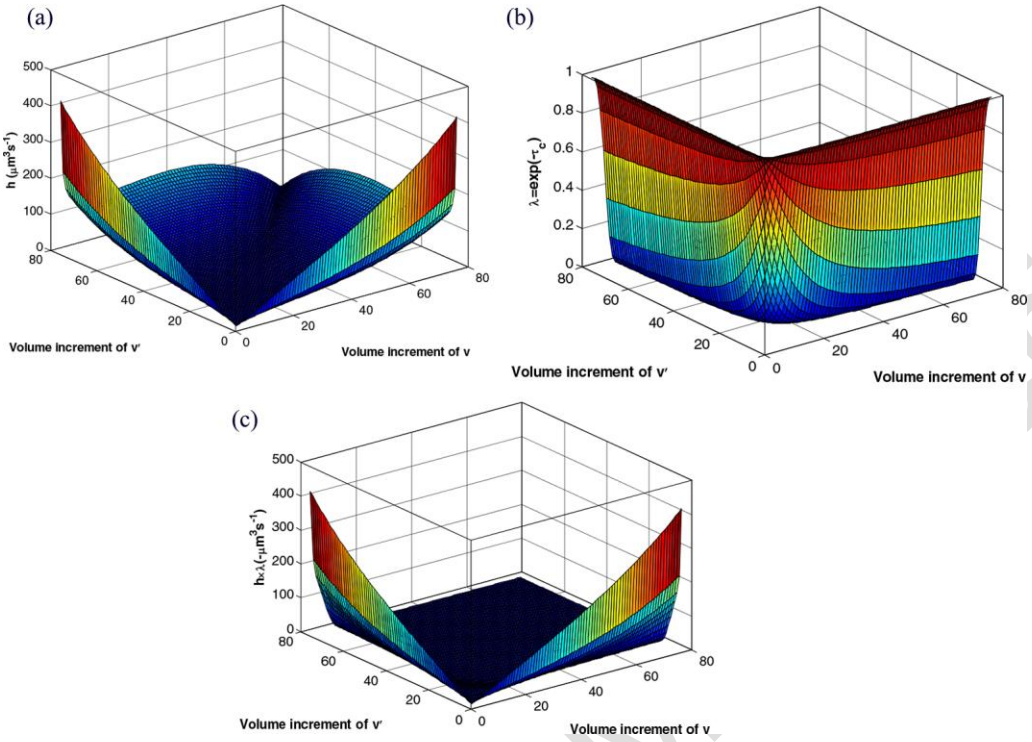

Figure 7. Effect of surface coverage of droplets on coalescence efficiency (a) Γ/Γ_{max}=0.44, (a) Γ/Γ_{max}=0.82.

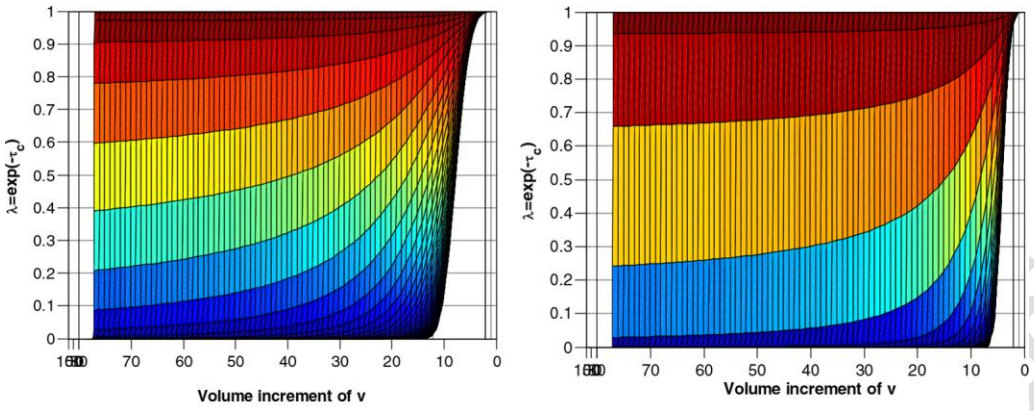

Figure 8. Average droplet size of sedimentation column after immobility.

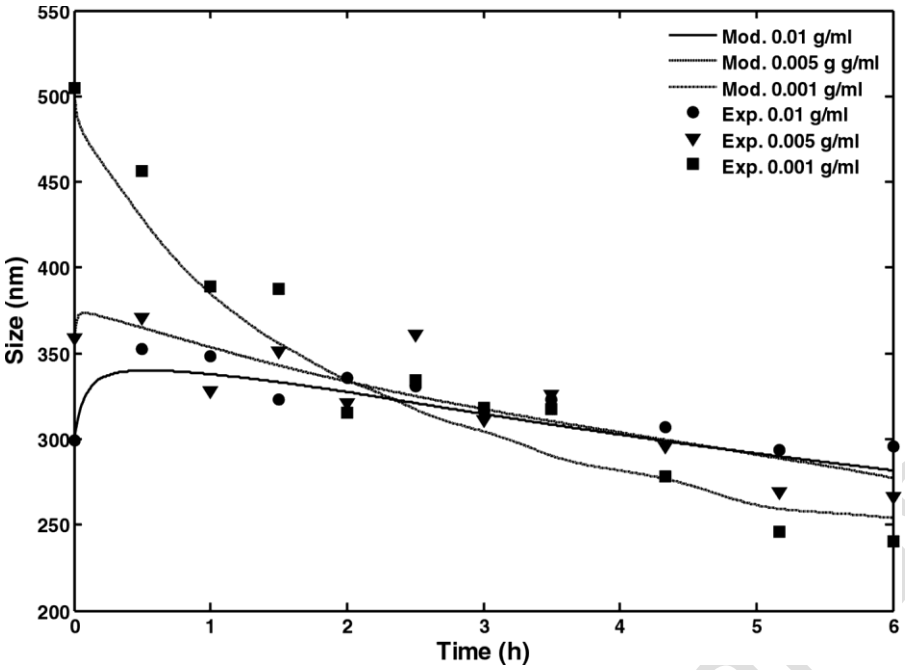

Figure 9. (a) Local volume fraction of emulsions after 2 hour immobility, (b) local volume fraction of emulsion containing 0.005 g/ml surfactants after 0, 2, 4 and 6 hours immobility.

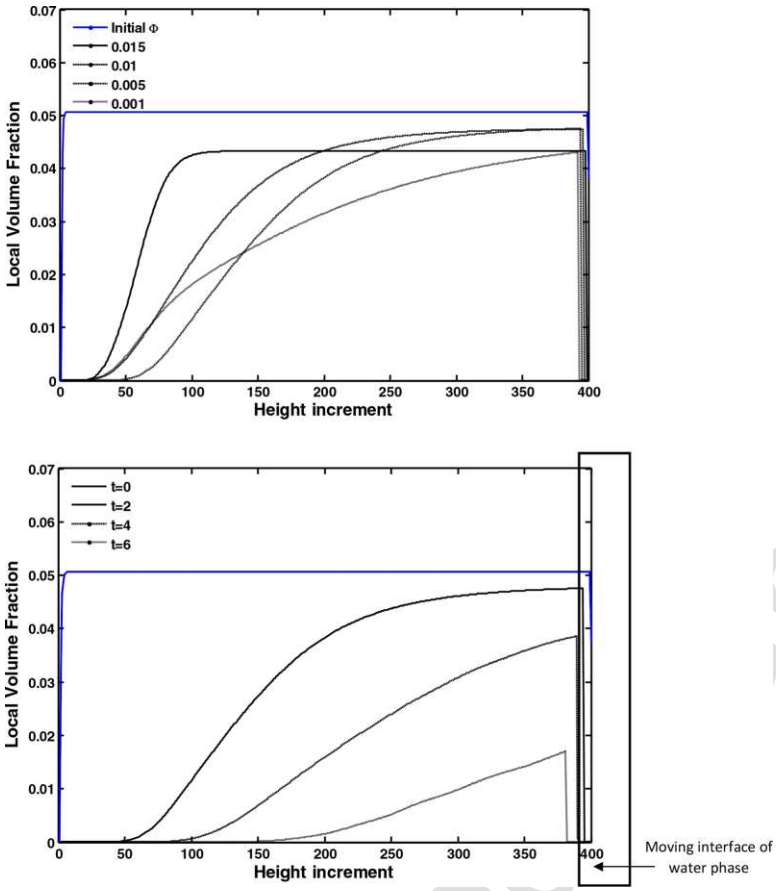

Figure 10. Different isotherm adsorptions which have been fitted by optimum surface coverage of droplets.

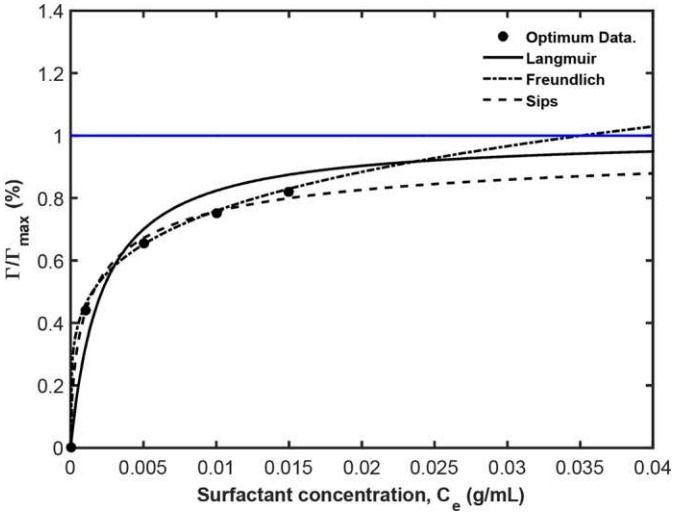

Figure 11. (a) water in oil emulsions at different surfactants concentration; (b) Average droplet size of emulsions versus surfactants concentration.

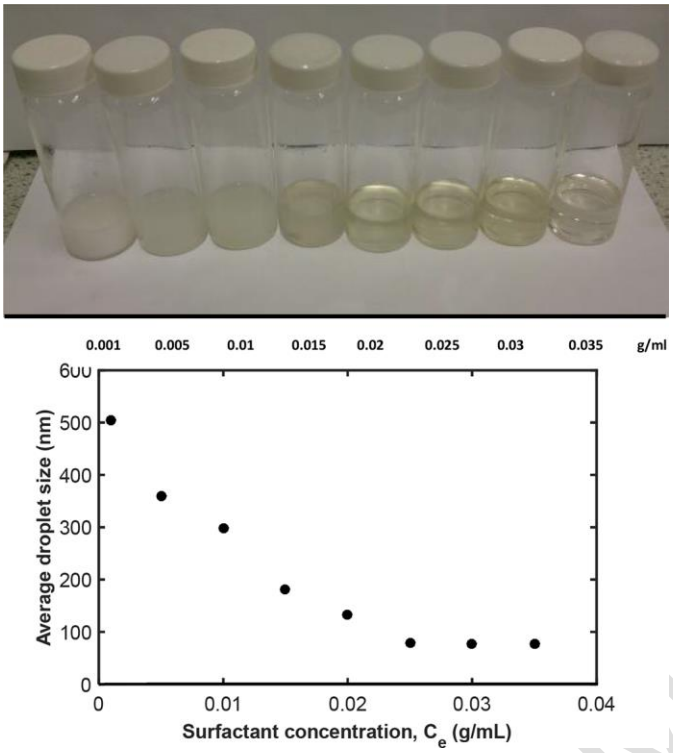

Figure 12. Interfacial tension of emulsion and de-ionized water.

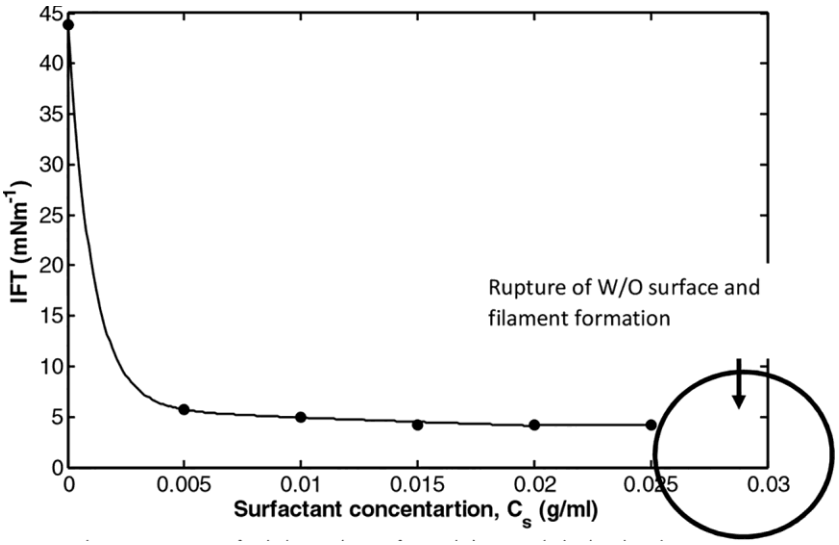

Figure 13. (a) Interfacial tension for (a) pure cyclohexane,IFT=42.1 mNm^{-1}(b) C_s=0.005 g/ml IFT=5.61 mNm^{-1}, (c) C_s=0.025 g/ml, IFT=4.19 mNm^{-1} (c) C_s=0.035 g/ml, No IFT measurement.